Bounding Pandemic Spread By Heat Spread

Teddy Lazebnik (lazebnik.teddy@gmail.com)
University College London https://orcid.org/0000-0002-7851-8147
Uri Itai
DataClue UK

Research Article

Keywords: partial-knowledge pandemic management, graph-based stochastic SIR model, diffusion rate boundary

Posted Date: June 2nd, 2022

DOI: https://doi.org/10.21203/rs.3.rs-1665680/v1

Bounding Pandemic Spread By Heat Spread

Teddy Lazebnik *[1,2] and Uri Itai[1]

[1]DataClue UK, London, UK
[2]Department of Cancer Biology, Cancer Institute, University College London, London, UK

Abstract

The beginning of a pandemic is a crucial stage for policymakers. Proper management at this stage can reduce overall health and economical damage. However, knowledge about the pandemic is insufficient. Thus, the use of complex and sophisticated models is challenging. In this study, we propose analytical and stochastic heat spread-based boundaries for the pandemic spread. These are compared with the stochastic Susceptible-Infected-Recovered (*SIR*) model taking place on an interaction graph. The proposed boundaries are not requiring accurate biological knowledge such as the *SIR* model does.

Keywords: partial-knowledge pandemic management, graph-based stochastic *SIR* model, diffusion rate boundary.

1 Introduction

Over the history of mankind, pandemics cause repetitive catastrophic suffering [1]. It cause significant increase in the mortality rate [2], major economic losses [3], and substantial political instability [4]. However, good management of the situation can significantly reduce all of this [5, 6]. Nonetheless, proper governance during a pandemic time requires an understanding of the pandemic's dynamics. Unfortunately, this task is very challenging. The main difficulty is the uncertainty in real-time. To reduce this, one needs to consider all the relevant factors. Nevertheless, pointing out the suitable features that appear in real-time is extremely hard [7]. The process of collecting epidemiological, clinical, and biological data is time-consuming, expensive, and complex at the operational level [8, 9]. In addition, policymakers need to act fast during the beginning of the pandemic to contain it at an early stage [10]. Inability to do so will result in greater disaster later in the pandemic.

Thus, providing policy-making good analytic tools is essential. The fashion to obtain data-driven decisions is epidemiological-mathematical models [11]. These provide an analytical framework to obtain an analysis of the pandemic's spread dynamics [12]. A large group of epidemiological models is based on the Susceptible-Infected-Recovered (SIR) model [7]. This model provides good baseline results [13]. The *SIR* model assumes that the course of an epidemic is short compared with the life of an individual. Therefore, the size of the population may be considered to be a constant. This assumption is reasonable as far as it is not modified by deaths due to the epidemic disease itself. Furthermore, the *SIR* model assumes all individuals in the population are initially equally susceptible to the disease (S) and only one individual is infected (I) at the beginning of the pandemic. Moreover, it further assumed that complete immunity is conferred by a single infection. In other words, it is possible to represent the *SIR* model using a system of non-linear ordinary differential equations where the average infected rate β and the average recovery rate γ are known:

$$\begin{aligned} \frac{dS(t)}{dt} &= -\beta S(t)I(t) \\ \frac{dI(t)}{dt} &= \beta S(t)I(t) - \gamma I(t) \\ \frac{dR(t)}{dt} &= \gamma I(t). \end{aligned} \tag{1}$$

*Corresponding author: lazebnik.teddy@gmail.com

Naively, one would consider the average infected rate β and the average recovery rate γ to be deterministic quantities that might cause model artifacts. For example, a susceptible individual ($p \in S$) can be infected and transformed into the infected sub-population (I) in a given time t. Immediately afterward, in time $t+1$, there is a probability γ that the same individual is recovered and transformed to the recovered sub-population (R) [14]. To overcome this, we considered these quantities to be stochastic. This is because the uncertain nature of multiple epidemiological, social, and economic processes produce these coefficients. Hence, it is possible to treat these coefficients as a transformation probability between the states [15].

To gain a more epidemiological detailed model, one can use an interaction graph to represent infection routes. From an epidemiological point of view, an interaction graph gives a more descriptive representation of infections between individuals [16]. Formally, an interaction graph is where individuals are the graph's nodes and the graph's edges are the possible infection routes. Indeed, Wang et al. [17] proposed a graph-based Susceptible-Infected-Susceptible (SIS) model. In their settings, each individual is represented as a node in a static, connected, and random graph. Similarly, Hau et al. [18] proposed an SEIR (E-exposed) model for sexually transmitted diseases. The authors defined the interactions between individuals using a bipartite static graph. These approaches are shown to well capture the pandemic spread dynamics. However, they still depend on a precise approximation of the infection and recovery rates [18]. This is due to the resilience problem in the ordinary differential equations [6].

Another possible approach to tackle the pandemic spread prediction task is using heat spread. The transformation of heat on manifold plays an important role in many fields of science and engineering [19, 20, 21]. Heat spread shown to be promising in both theoretical [22, 23] and practical settings [24, 25]. The heat spread can be represented using the following partial differential equation:

$$\frac{\partial u(t,\bar{x})}{\partial t} = c\Delta u(t,\bar{x}), \tag{2}$$

where t is the time, $\bar{x}$ is an n-dimensional space, and $c \in \mathbb{R}^+$ is the diffusion coefficient. A discrete version of the heat spread equations takes the form:

$$\frac{\partial u(t,\bar{x})}{\partial t} = c\Sigma_{i=0}^{n} \frac{\partial^2 u(t,\bar{x})}{\partial x_i^2}, \tag{3}$$

such that

$$\frac{\partial u(t,\bar{x})}{\partial t} := \frac{u(t+h,\bar{x}) - u(t,\bar{x})}{h}$$

and

$$\frac{\partial u(t,\bar{x})}{\partial x_i} := \frac{u(t,[x_1,\ldots,x_i+h,\ldots x_n]) - u(t,[x_1,\ldots,x_i,\ldots x_n])}{h},$$

where $h \in \mathbb{R}^+ \backslash \{0\}$ [26].

Graphs are locally, on the node-level, isometric to manifold with a dimensional corresponding to the number of neighbors of the center node. Hence, assuming a graph $G := (V, E)$, the heat spread dynamics for each node $v \in V$ agrees with Eq. (3) such that $h = 1$ and $n = |\{v_i \in V \mid (v, v_i) \in E\}|$.

Following this, one can conclude that knowledge is required to obtain a fine approximation of the heat spread in an interaction graph. Specifically, only information on the interaction between individuals is needed. While the stochastic graph-based *SIR* model is based on a more precise biological, social, and epidemiological knowledge. This information is not necessarily available during the beginning of a pandemic.

To fill this gap, we propose two upper boundaries for the pandemic spread in the population. Our method is based on the heat spread on interaction graphs. This allows us to provide policymakers a range of insights based on the connection between the two. This paper is organized as follows: in Section 2, we present two upper boundaries (*maximum* and *mean*) of a stochastic graph-based *SIR* model using the heat spread. In Section 3, we evaluate the usefulness of the proposed boundaries in a k-regular and random graphs. Following this, we evaluate the boundaries on social network data from Facebook to simulate realistic interaction graph settings. In Section 4, we discuss the possible epidemiological usage of these boundaries with their limitations and propose future work.

2 Pandemic Spread Bounded By Heat Spread

As mention above, one can consider the pandemic spread as diffusion on a graph. Locally this is equivalent to the heat equation on a graph. Since a graph is a manifold we have a local coordinate system. Thus, we can locally apply heat transform on a k dimensional grid.

To formalize the heat equation on a single node, one needs to calculate the probability of the node to be *infected*. The probability a node i with $|N_b(i)|$ adjacent nodes would be infected is corresponding to the probability that each infected adjacent node ($v_j \in N_b(i)$) would infect node i.

$$p_i(\text{infected}) := 1 - \prod_{j \in N_b(i)} \big(1 - p_j(\text{infected})\big), \tag{4}$$

such that $p_j(\text{infected}) = 0$ if node j is not infected and some probability $p \in (0, 1]$ otherwise. We note that form Eq. (4) we get that the rate of infected grows exponentially towards one.

Based on this dynamics, we formally define the epidemiological interaction graph as follows. Let $G := (V, E)$ be a underacted, connected graph such that $E \subset V \times V$ and $|V| = N$. Each node $v \in V$ is representing an individual in the population. A node is defined by a finite state machine with three states $\{S, I, R\}$ - corresponding to the *SIR* model's states. In addition, the edge $e = (v_i, v_j) \in E$ is a possible interaction between two individual $v_i, v_j \in V$.

Following this, a stochastic *SIR* on an infected graph can be defined as follows. Given an infected graph (G) and the parameters $\beta, \gamma \in (0, 1]$. At a given point in time, if $v_j \in N_b(v_i) \wedge v_j \in S \wedge v_i \in I$, than v_j infected. Viz, v_j transforms to state I at a probability β. In addition, if $v_i \in I$ than v_i recover. Namely, transforms to state R at a probability γ. The process is terminated when I reaches zero. Lazebnik et al. [14] had proved that the only recurrent state for the stochastic *SIR* model is $(S, I, R) = (N - d, 0, d)$ such that $1 \leq d \leq N$. Thus, the asymptotically state of the dynamics is achieved when $I = 0$. Therefore, the process halts.

Akin, one can define the heat spread on an infected graph can as follows. Given an infected graph (G) and the parameter $c \in \mathbb{R}^+$. At a given point in time, if $v_j \in N_b(v_i) \wedge v_j \in S \wedge v_i \in I$, then v_j become infected. That is, v_j transforms to state I) after $\lceil \frac{1}{c} \rceil$ time steps. Moreover, if $v_i \in I$ then v_i recovered. Namely, transforms to state R if $\forall v_j \in N_b(v_i)$ such that $v_j \in I$. The process is terminated when I reaches zero. By treating the dynamics as a Markovian process [27], one can notice that the only recurrent state of the process takes the form $(S, I, R) = (0, 0, N)$. This happens because all individuals would eventually infected and recover. Hence, the asymptotically state of the dynamics is achieved when $I = 0$. Consequently, the process halts.

Based on these definitions, given an interaction graph that representing a population, one can bound the pandemic spread according to the stochastic *SIR* model using the heat spread model as shown in Theorem 1.

Theorem 1. *Given an infected graph (G) with infection rate $\beta \in (0, 1]$ and recovery rate $\gamma \in (0, 1]$. In addition, assuming the initial condition $(S, I, R) = (N - 1, 1, 0)$. Than, exists a diffusion rate $c \in \mathbb{R}^+$ that agrees with:*

$$\forall t \in \mathbb{N} : R_0^{SIR(\beta,\gamma)}(t) \leq R_0^{Diffusion(c)}(t). \tag{5}$$

Proof. Let v_0 be the node which satisfies $v \in I$ at $t = 0$. Node v_0 is a single node according to the assumptions. Performing a breadth-first search (BFS) [28] starting from v_0. During the BFS, each node $v \in G$ has been allocated with a distance d from v_0. On one hand, for the stochastic *SIR* process, the worst case scenario obtained where $\beta = 1$ and $\gamma = \epsilon > 0$. This is happens as larger β and smaller γ increase the pandemic spread. In this case,

$$R_0^{SIR(\beta,\gamma)} \leq R_0^{SIR(1,\epsilon)} \leq \max_{k \in [1,N-1]}(|\{v \in V \mid d(v_0, v_i) = k\}|). \tag{6}$$

By setting the diffusion rate c to be $\max_{k \in [1,N-1]}(|\{v \in V \mid d(v_0, v_i) = k\}|)$, for any infection rate $\beta \in (0, 1]$ and recovery rate $\gamma \in (0, 1]$, the condition

$$\forall t \in \mathbb{N} : R_0^{SIR(\beta,\gamma)}(t) \leq R_0^{Diffusion(c^*)}(t), \tag{7}$$

satisfied.

□

A corollary of Theorem 1 is that the pandemic spread and heat spread are isomorphic where $\beta = c = 1$ and $\gamma = 0$. This is true since, the processes are defined to be isomorphic if and only if $\forall t \in \mathbb{N} : |\{v \in V \mid v \in I\}|$ is identical for both processes. Using the definition of the *event horizon*, one can immediately notice that.

Definition 2.1. The *event horizon* is the set of nodes H which satisfies:

$$H := \{v \in V \mid v_j \in N_b(v_i) : v_j \in I \wedge v_i \in S\}$$

Following this, one can point out that, at time $t = 0$ in both processes the size of infected nodes depends on the interaction graph. For each step in time, the event horizon $H \subset V$ is infected while the other nodes are not. This means both processes are deterministically identical for $\beta = c = 1$ and $\gamma = 0$.

While this boundary holds for any pandemic, we note that this boundary is not tied for the most realization of a pandemic. This is due to the high variance in the pandemic spread [29, 30, 11]. Therefore, one can bound the mean pandemic spread given the interaction graph, as shown in Theorem 2. The mean pandemic spread provides a more tied boundary of the pandemic spread given only the infection rate β.

Theorem 2. *Given an infected graph (G) with infection rate $\beta \in (0, 1]$ and recovery rate $\gamma \in (0, 1]$. In addition, assuming the initial condition $(S, I, R) = (N - 1, 1, 0)$. The vector of mean infection time (V_j^i) agrees with the minimal (e.g., if x_j is another solution with $x_j \geq 0$ then $x_j \geq V_j$) non-negative solution of the following equation:*

$$\begin{cases} V_j^i = \frac{1}{\beta} + \Sigma_{k \neq j} \beta V_k^i, \ i \neq j \\ V_j^i = 0, \ otherwise \end{cases}, \tag{8}$$

where $V_j^i \in \mathbb{N} \cup \infty$ is a random variable that stands for the time pass that an infection that starts at individual i will infect individual j. We define the hitting time of a state $i \in V$ as a random variable $H^i : V \to \mathbb{N} \cup \infty$ given by

$$H^i(v) = inf\{n \geq 0 : X_n(v) = i\}.$$

Proof. First, we show that V_j^i satisfies Eq. (8). If $i = j$ than $H^i = 0$ by definition and therefore $V_j^i = 0$. If $i \neq j$, than $H^i \geq 1$. According to the Markov property,

$$E_i(H^i | X_1 = j) = \frac{1}{\beta} + E_j(H^i).$$

and

$$V_j^i = E_j(H^i) = \Sigma_{k \in V} E_i(H^i 1_{X_1 = k}) = \Sigma_{k \in V} E_i(H^i | X_1 = k) P_i(X_1 = k) = \tfrac{1}{\beta} + \Sigma_{k \neq j} \beta V_k^i. \tag{9}$$

Suppose that y is any solution to Eq. (8). Than, for $i = j$, $V_j^i = y = 0$. If $i \neq j$,

$$y = \tfrac{1}{\beta} + \Sigma_{k \neq j} \beta y_k = \tfrac{1}{\beta} + \Sigma_{k \neq j} \beta \big(1 + \Sigma_{l \neq j} (\beta y_{k,l})\big) = P(H^i \geq 1) + P(H^i \geq 2) + \dots \tag{10}$$

By repeating this substitution for y, in the final term (after n steps) we obtain

$$y \geq P(H^i \geq 1) + \dots P(H^i \geq n) \tag{11}$$

and, letting $n \to \infty$,

$$y \geq \Sigma_{n=1}^{\infty} P(V_j^i \geq n) = V_j^i. \tag{12}$$

□

Example 1. In the *ladder* graph, as illustrated in Fig. 1, the inequality in Eq. (8) is sharp. For that, we need two insights. The first one is that each infection path is independent. Namely, if one path is is faster or slower it is orthogonal to any other path. The second is that there exists a positive probability realization that the node would be infected by another path than the shortest probability path. This implies that when one calculates the expected infected time, he would get a lower time than taking only the shortest path.

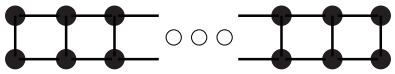

Figure 1: A schematic view of a *ladder* graph.

Corollary 2.1. For a given infected graph and a fixed infection rate $\beta \in (0,1)$ and recovery rate $\gamma \in (0,1)$. If one will add an infected path the infection rate would strictly increase.

We note that for a single adjacent node the boundary in Eq. (8) is tight. It can be monotonically relaxed by increasing the number of adjacent nodes, γ, and β.

According to Theorem 1 and 2, for $\beta = c$ and $\gamma = 0$ then the processes are converging to the same mean. Thus, in the case $\gamma > 0$, the heat spread with diffusion rate $c = \beta$ is an upper boundary of the mean case of the stochastic *SIR* dynamics. This outcome can be obtained by computing the mean infection time from the first infected individual to any other individual in the population. Following this step, one needs to compute the inverse value for this quanta to obtain the mean pandemic spread rate. Nonetheless, to use this boundary requires a good approximation of the infection rate (β). Otherwise, the boundary may be either too high or too low. In the case of the first boundary (Eq. (5)), such knowledge is not required.

3 Numerical Simulations

In the above, we develop theoretical bounds on the pandemic spread. In addition, we had shown that these bounds are not tight for some cases. In this section, we will present numerical simulations of such models. We numerically examine the spread dynamics on several graphs types. For each graph, we calculate the stochastic *SIR* spread and associated heat spread models.

In particular, k-regular graphs, random graphs, and a real-world social interaction graph. We computed the pandemic spread with infection rate of $\beta = 0.07$ and recovery rate of $\gamma = 0.07$. These values were chosen to represent the COVID-19 pandemic [30]. Additionally, according to Theorems 1 and 2 the *maximum* and *mean* diffusion rates are set to be 1 and 0.07, respectively.

First, we obtain the connection between the k-regularity of a graph and the pandemic spread. In plain English, we computed the mean basic reparation number of the pandemic. We choose this metric because it is commonly considered to be the proper metric to measure overall pandemic spread [31]. We randomly generated $n = 10$ k-regular, connected graphs with $|V| = 1000$. The results of this process are presented in Fig. 2. Where the x-axis is the value of k and the y-axis is the mean basic reparation number.

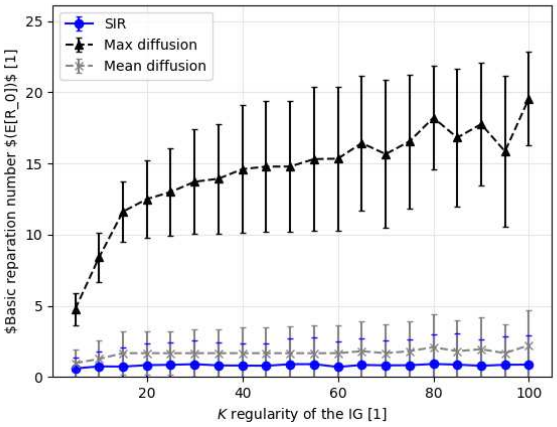

Figure 2: The mean basic reproduction number as a function of the k-regularity of the interaction graph. The values provided for the stochastic *SIR* model (blue circles), mean diffusion boundary (gray axis), and maximum diffusion boundary (black triangles). Each sample is shown as mean $\pm$ standard deviation for $n = 10$.

Since interaction graphs are not necessarily k-regular, we computed the mean basic reproduction number for connected, random graphs. The graphs were randomly generated such that each node $v \in V$ has between 3 and 200 edges, in a uniform distribution. We generated 100 samples for graphs at size $|V| = 1000$. The results of this process are presented in Fig. 3. Where the x-axis is the number of edges in the graph ($|E|$) and the y-axis is the mean basic reparation number.

The above graphs were constructed synthetically. Thus, a natural question that rise is "does this model words on real-life graphs?". To answer this question, we tested the model on the Facebook interaction graph.

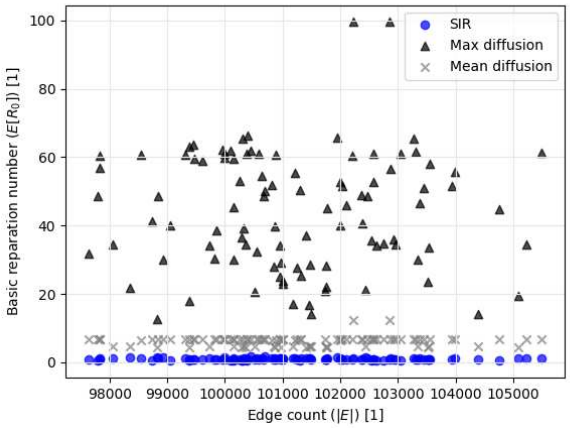

Figure 3: The mean basic reproduction number as a function of the interactions graph's connectivity (e.g., $|E|$). The values for the stochastic*SIR* model, mean diffusion boundary, and maximum diffusion boundary are provided.

This graph represents the friendships between individuals in the Facebook social platform [32]. In addition, it contains $|V| = 4039$ nodes and $|E| = 176,468$ edges (1.01% density). Moreover, each node $v \in V$ has 44 ± 52 neighbors. A histogram of the number of neighbors per node is provided in the supplementary material. We calculated the pandemic spread for the maximum heat spread boundary, the mean heat spread boundary, and the stochastic *SIR* model, as shown in Figs. 4a, 4b, and 4c, respectively.

4 Discussion

Estimating the infection rate is critical information for pandemic management [18, 7]. In this paper, we showed boundaries on the infection rate. By using the heat spread dynamics with different diffusion rates we learned that the rate is highly dependent on the topology of the interaction graph. The boundaries of a stochastic *SIR* model's infection rate were assumed to take place on an interaction graph. This provides a better representation of the epidemiological dynamics in a heterogeneous population. Health professionals would benefit from the representation we provide. Since the proposed boundaries are relatively easy to obtain as they require almost no prior data. Specifically, we presented the *worst case* (also called the *maximum case*) and the *mean case* pandemic spread boundaries. This is especially useful at the beginning of a pandemic since acting fast can significantly reduce overall infection [10]. For example, during the COVID-19 pandemic [33], the infection and recovery rates were rapidly update [30, 13, 34, 35, 36]. This led to large errors in the estimations of the pandemic spread. As a result, policymakers provided with a distorted image. Hence, the proposed boundaries provide an initial solution. Once more data is gathered, one would be able to both improve the proposed boundaries and use more sophisticated and adjusted models.

The *maximum* heat spread boundary is deterministic tight. Therefore, it cannot be improved. Nonetheless, this case represent a catastrophic scenario where $\beta = 1, \gamma = 0$. This case may cause unnecessary panic and extreme reactions. Obviously, these are not necessarily required to contain the pandemic spread. However, if slightly more information is provided such as the approximation of the infection rate (β), one can obtain a better approximation of the infection spread rate. Indeed, in such a case, we can use the *mean* heat spread boundary. This boundary provides a tighter approximation to the stochastic *SIR* model. This is done without knowing the recovery rate or anything on the interaction graph, as shown in Fig. 3. Withal, the *mean* heat spread boundary is constituent in providing a mean boundary over the stochastic *SIR*. This is significantly less than the *maximum* heat spread boundary over different levels of connectivity in the population, as shown in Fig. 2. In fact, when applied to the Facebook interaction graph [32], the *maximum* and *mean* heat spread boundaries provided 20 and 1.66 times greater pandemic spread rate on average compared to the stochastic *SIR* model, as shown in Fig. 4.

The usage of heat spread as the boundary for the pandemic spread is useful in real settings. This is

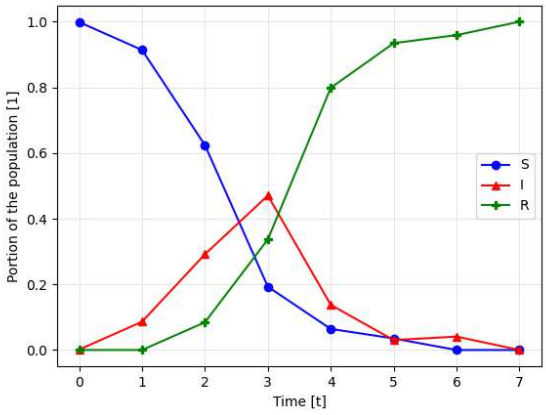

(a) Maximum heat spread ($c = 1$) boundary.

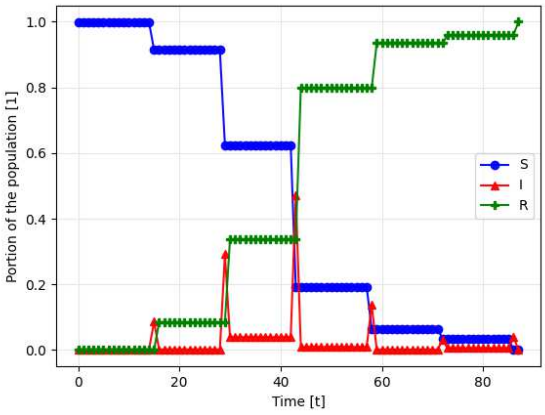

(b) Mean heat spread ($c = \beta$) boundary.

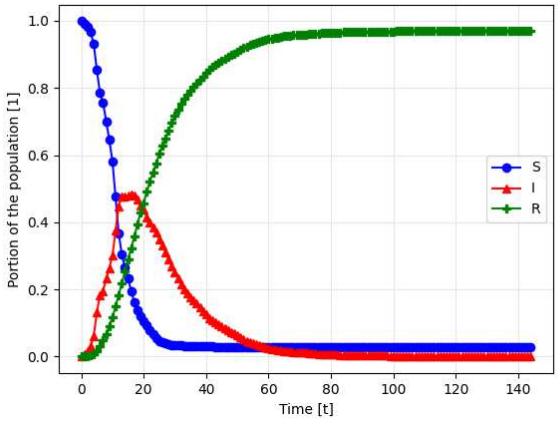

(c) The stochastic *SIR* model.

Figure 4: The pandemic spread over time for the Facebook [32] interaction graph.

because one can find the diffusion rate c from local infection spread. By computing only the infection rate of interactions of infected individuals with their immediate environment. For comparison, this method does not work for obtaining the infection rate (β) and recovery rate (γ). Therefore, it is faster and more feasible to obtain the heat spread boundaries to the pandemic rather than the *SIR*-based pandemic spread.

A possible future work can be removing the assumption that the interaction graph is static over time. Specifically, one can allow the edges of the graph to change according to some socio-epidemiological logic. This relaxation would lead to a better representation of the pandemic spread in a population. As a result, this can reveal even better boundaries to the pandemic spread.

References

[1] A. A. Conti. "Historical and methodological highlights of quarantine measures: from ancient plague epidemics to current coronavirus disease (COVID-19) pandemic". In: *Acta bio-medica : Atenei Parmensis* 91.2 (2020), pp. 226–229.

[2] J. R. Goldstein and R. D. Lee. "Demographic perspectives on the mortality of COVID-19 and other epidemics". In: *PNAS* 117.36 (2020), pp. 22035–22041.

[3] H. Herrera, G. Ordonez, M. Konradt, and C. Trebesch. "Corona Politics: The Cost of Mismanaging Pandemics. PIER Working Paper No. 20-033". In: *SSRN* (2020).

[4] A. Roberts. “Pandemics and Politics”. In: *Survival* 62.5 (2020), pp. 7–40.

[5] T. Lazebnik, L. Shami, and S. Bunimovich-Mendrazitsky. “Pandemic Management by a Spatio-temporal Mathematical Model”. In: *International Journal of Nonlinear Sciences and Numerical Simulation* (2021).

[6] C. Vinay, H. Vikas, G. Sakshi, G. Adit, G. Mohsen, and S. Biplab. “Disaster and Pandemic Management Using Machine Learning: A Survey”. In: *IEEE Internet of Things Journal* (2020), pp. 1–1.

[7] W. O. Kermack and A. G. McKendrick. “A contribution to the mathematical theory of epidemics”. In: *Proceedings of the Royal Society* 115 (1927), pp. 700–721.

[8] T. H. Davenport, A. B. Godfrey, and T. C. Redman. “To Fight Pandemics, We Need Better Data”. In: *MIT Sloan Management Review* 62.1 (2020), pp. 1–4.

[9] A. Corsi, F. F. de Souze, R. N. Pagani, and J. L. Kovaleski. “Big data analytics as a tool for fighting pandemics: a systematic review of literature”. In: *Journal of Ambient Intelligence and Humanized Computing* (2020).

[10] T. P. T. Tran, T. H. Le, T. N. P. Nguyen, and V. M. Hoang. “Rapid response to the COVID-19 pandemic: Vietnam government’s experience and preliminary success”. In: *Journal of global health* 10.2 (2020), p. 020502.

[11] W. Yang, D. Zhang, L. Peng, C. Zhuge, and L. Liu. “Rational evaluation of various epidemic models based on the COVID-19 data of China”. In: *medRxiv* 344 (2020).

[12] S. F. Darabi and C. Scoglio. “Epidemic spread in human networks.” In: *50th IEEE Conference on Decision and Control and European Control Conference*. 2011, pp. 3008–3013.

[13] O. Ifguis, M. El Ghozlani, F. Ammou, A. Moutcine, and Z. Abdellah. “Simulation of the Final Size of the Evolution Curve of Coronavirus Epidemic in Morocco using the SIR Model”. In: *Journal of Environmental and Public Health* (2020).

[14] T. Lazebnik, S. Bunimovich-Mendrazitsky, and L. Shaikhet. “Novel Method to Analytically Obtain the Asymptotic Stable Equilibria States of Extended SIR-type Epidemiological Models”. In: *Symmetry* (2021).

[15] J-C. Cortés, S. K. El-Labany, A. Navarro-Quiles, M. M. Selim, and H. Slama. “A comprehensive probabilistic analysis of approximate SIR-type epidemiological models via full randomized discrete-time Markov chain formulation with applications”. In: *Mathematical Methods in the Applied Sciences* 43.14 (2020), pp. 8204–8222.

[16] C. J. Noakes, C. B. Beggs, P. A. Sleigh, and K. G. Kerr. “Modelling the transmission of airborne infections in enclosed spaces”. In: *Epidemiol. Infect.* 134 (2006), pp. 1082–1091.

[17] X. Wang, Z. Wang, and H. Shen. “Dynamical analysis of a discrete-time SIS epidemic model oncomplex networks”. In: *Applied Mathematics Letters* 94 (2019), pp. 292–299.

[18] H-F. Huo, Q. Yang, and H. Xiang. “Dynamics of an edge-based SEIR model for sexually transmitted diseases”. In: *Mathematical Biosciences and Engineering* 17 (2019), pp. 669–699.

[19] W. M. Yu and W. Xiaoming. “PDE-Driven Level Sets, Shape Sensitivity and Curvature Flow for Structural Topology Optimization”. In: *CMES - Computer Modeling in Engineering and Sciences* 6.4 (2004), pp. 373–395.

[20] J. Cerda, A. W. Westerberg, D. Mason, and B. Linnhoff. “Minimum utility usage in heat exchanger network synthesis A transportation problem”. In: *Chemical Engineering Science* 38.3 (1983), pp. 373–387.

[21] T. Dbouk. “A review about the engineering design of optimal heat transfer systems using topology optimization”. In: *Applied Thermal Engineering* 112 (2017), pp. 841–854.

[22] K. D. Cole, M. R. Yavari, and P. K. Rao. “Computational heat transfer with spectral graph theory: Quantitative verification”. In: *International Journal of Thermal Sciences* 153 (2003), p. 106383.

[23] I. Naveros, C. Ghiaus, J. Ordonez, and D. P. Ruiz. “Thermal networks considering graph theory and thermodynamics”. In: *12th International Conference on Heat Transfer, Fluid Mechanics and Thermodynamics 2016* (2016).

[24] H. E. Anderson. “Heat transfer and fire spread”. In: *Res. Pap. INT-RP-69. Ogden, Utah: U.S. Department of Agriculture, Forest Service, Intermountain Forest and Range Experiment Station* (1969), p. 20.

[25] K. M. Brydena, D. A. Ashlockb, D. S. McGregory, and G. L. Urbana. "Optimization of heat transfer utilizing graph based evolutionary algorithms". In: *International Journal of Heat and Fluid Flow* 21.2 (2003), pp. 267–277.

[26] B. Fornberg. "Numerical Differentiation of Analytic Functions". In: *ACM Trans. Math. Softw.* 7.4 (1981), pp. 512–526.

[27] N. Privault. *Understanding Markov Chains*. Springer Singapore, 2018.

[28] E. F. Moore. "The shortest path through a maze". In: *Proceedings of the International Symposium on the Theory of Switching* (1959), pp. 285–292.

[29] S. Bunimovich-Mendrazitsky and L. Stone. "Modeling polio as a disease of development". In: *Journal of Theoretical Biology* 237 (2005), pp. 302–315.

[30] T. Lazebnik and S. Bunimovich-Mendrazitsky. "The signature features of COVID-19 pandemic in a hybrid mathematical model - implications for optimal work-school lockdown policy". In: *advanced theory and simulations* (2021).

[31] Y. Alimohamadi, M. Taghdir, and M. Sepandi. "Estimate of the Basic Reproduction Number for COVID-19: A Systematic Review and Meta-analysis". In: *Journal of preventive medicine and public health* 53.3 (2020), pp. 151–157.

[32] J. McAuley and J. Leskovec. "Learning to Discover Social Circles in Ego Networks". In: (2012).

[33] Eurosurveillance Editorial Team. "Note from the editors: World Health Organization declares novel coronavirus (2019-nCoV) sixth public health emergency of international concern". In: *Euro Surveill* 25 (2020), 200131e.

[34] J. Chen, T. Qi, L. Liu, Y. Ling, Z. Qian, and T. Li. "Clinical progression of patients with COVID-19 in Shanghai, China". In: *The Journal of infection* (2020).

[35] J.R. Lechien, C.M. Chiesa-Estomba, S. Place, Y. Van Laethem, P. Cabaraux, and Q Mat. "Clinical and epidemiological characteristics of 1420 European patients with mild-to-moderate coronavirus disease 2019". In: *J Intern Med* (2020).

[36] J. Wu, W. Li, X. Shi, Z. Chen, B. Jiang, and J. Liu. "Early antiviral treatment contributes to alleviate the severity and improve the prognosis of patients with novel coronavirus disease (COVID-19)". In: *J Intern Med* (2020).

Supplementary Files

This is a list of supplementary files associated with this preprint. Click to download.

- appendix.pdf